Available online at www.sciencedirect.com
SCIENCE DIRECT
Journal of Photochemistry and Photobiology A: Chemistry 172 (2005) 97–107
Journal of Photochemistry and Photobiology A:Chemistry
www.elsevier.com/locate/jphotochem

Synthesis, characterization, and optical properties of a cyano-functionalized 2,3,7,8-tetraaryl-1,6-dioxapyrene

Daniel S. Tyson[a,b], Eve F. Fabrizio[a,b], Matthew J. Panzner[c], James D. Kinder[a], Jean-Pierre Buisson[d], Jørn B. Christensen[e], Michael A. Meador[a,*]

[a] *Polymers Branch, Materials Division, NASA Glenn Research Center, Cleveland, OH 44135, USA*
[b] *Ohio Aerospace Institute, Cleveland, OH 44142, USA*
[c] *Department of Chemistry, The University of Akron, Akron, OH 44325, USA*
[d] *Service de Chimie, Institut Curie, 26 rue d'Ulm, 75248 Paris Cedex 05, France*
[e] *Chemical Laboratory II, University of Copenhagen, DK-2100 Copenhagen Ø, Denmark*

Received 8 October 2004; received in revised form 22 November 2004; accepted 24 November 2004
Available online 29 January 2005

Abstract

2,7-Di(4-cyanophenyl)-3,8-di(4-methylphenyl)-1,6-dioxapyrene (*CN-diox*), a symmetrically substituted 2,3,7,8-tetraaryldioxapyrene, was synthesized in seven steps from 1,5-dihydroxynaphthalene. The synthetic methodology incorporated a base-catalyzed ring closure process followed by dehydration to introduce the first tetraaryl-1,6-dioxapyrene. Crystal structure and electrochemical analysis were performed to directly compare the properties of *CN-diox* to previously reported dioxapyrene derivatives, specifically 1,6-dioxapyrene (*Diox*) and 3,8-diethyl-5,10-dimethyl-1,6-dioxapyrene (*Alkyl-diox*). Optical spectroscopy studies were performed to evaluate the potential of the 1,6-dioxapyrenes as fluorescent probes. *CN-diox* revealed a broad absorption centered near 450 nm ($\varepsilon = 31{,}900\ M^{-1}\ cm^{-1}$) in THF with a corresponding fluorescence at 619 nm ($\Phi_f = 0.011$). This was in sharp contrast to both *Diox* and *Alkyl-diox* which displayed broad absorption bands near 400 nm ($\varepsilon \sim 5000$–$10{,}000\ M^{-1}\ cm^{-1}$) in THF with corresponding fluorescence near 500 nm ($\Phi_f = 0.059$ and 0.082 for *Diox* and *Alkyl-diox*, respectively). The luminescence of *CN-diox* was found to be solvatochromic ($\lambda_{max} = 619$–644 nm) with single exponential lifetimes of less than 1.3 ns and an excited state dipole moment of ∼22.81 D. Neither *Diox* nor *Alkyl-diox* showed solvatochromic properties.

Keywords: 1,6-Dioxapyrene; Synthesis; Electronic spectra; Luminescence; Electrochemistry; Solvatochromism

1. Introduction

Since the original reports on the synthesis and properties of 1,6-dioxapyrenes in the early 1990s [1–3], there have been numerous derivatives prepared [1–5] along with studies reporting crystal structures [6,7], detailed NMR characterization [8,9], applications as conductive salts [10], spectroscopic properties [11], and molecular orbital calculations [12]. 1,6-Dioxapyrenes have generally been prepared by acid or base-catalyzed ring closures from substituted naphthalenes. The present work enhances the traditional methodology of base-catalyzed ring closure and introduces the first tetraaryl-1,6-dioxapyrene.

Our group has been working toward developing visible/near IR solvatochromic dyes for future NASA planetary exploration missions (for example, as polymeric and biological probes). Previous work has introduced a series of substituted, symmetrical and unsymmetrical, benzodifurans that show high quantum efficiency and large solvatochromic response with respect to their emission spectra [13]. The favorable properties of these emissive chromophores is a result of charge transfer excited states that stem from the electron

* Corresponding author. Tel.: +1 216 433 9518; fax: +1 216 977 7132.
E-mail addresses: daniel.s.tyson@grc.nasa.gov (D.S. Tyson), michael.a.meador@grc.nasa.gov (M.A. Meador).

1010-6030/$ – see front matter © 2004 Elsevier B.V. All rights reserved.
doi:10.1016/j.jphotochem.2004.11.012

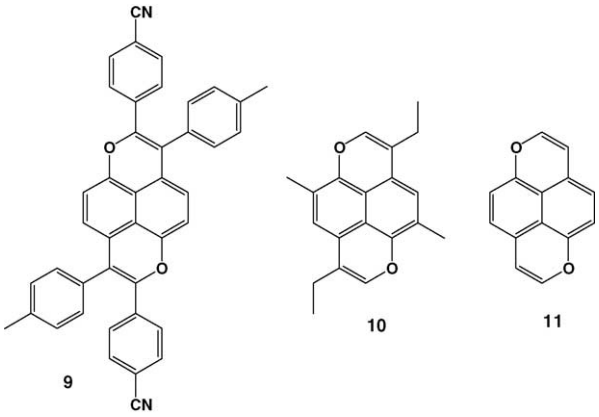

Fig. 1. *CN-diox* (**9**), *Alkyl-diox* (**10**), and *Diox* (**11**).

donating/accepting ability of the pendant groups [13]. In an effort to concomitantly extend the conjugation and increase the absorption/emission wavelength of our benzodifurans, we turned to dioxapyrenes.

Earlier reports indicated that substituted 1,6-dioxapyrenes could be synthesized in *real* quantities (i.e. hundreds of milligrams or more, enough to do thorough studies) and maintained visible emission [1–5,11]. Using the foundation outlined above, a dual approach was chosen. The first goal was to develop new or different routes to substituted 1,6-dioxapyrenes with either electron donating or electron accepting properties. The second goal was to measure the spectroscopic properties and evaluate the solvatochromic response of these compounds. We report herein the total synthesis and spectroscopic properties of the first symmetrically substituted, cyano-functionalized 2,3,7,8-tetraaryl-1,6-dioxapyrene (**9** or *CN-diox*, Fig. 1). All experiments were performed in direct comparison to unsubstituted [14] 1,6-dioxapyrenes (**10** or *Alkyl-diox* and **11** or *Diox*, Fig. 1) in order to clearly convey the unique spectroscopic properties of *CN-diox* (**9**).

2. Experimental

2.1. Materials and characterization

1,6-Dioxapyrene (**11** or *Diox*) and 3,8-diethyl-5,10-dimethyl-1,6-dioxapyrene (**10** or *Alkyl-diox*) were prepared as previously described [1,3]. All solvents and reagents were purchased from Aldrich and used as received. ^{1}H and ^{13}C NMR spectra were obtained on a Bruker AC 200 or Avance 300 MHz spectrometer. $CDCl_3$ or d_6-DMSO containing up to 1% TMS as an internal reference was used as the solvent for solution phase experiments. Mass data was measured on a Finnegan LCQ (atmospheric pressure ionization) in positive or negative ion mode with an inlet temperature of 180–220 °C. Normal phase HPLC was performed with a Hewlett-Packard HPLC system equipped with a diode array absorption detector or an Alliance HPLC system equipped with a dual channel absorption detector. Elemental analysis was obtained by Atlantic Microlabs, Inc. (Norcross, GA).

2.2. Crystallographic analysis

Crystals of *CN-diox* (**9**) were grown from slow concentration of a chloroform/dichloromethane solution. Data was collected on a Bruker Apex CCD diffractometer with graphite-monochromated Mo Kα radiation (λ = 0.71073 Å). Unit cell determination was achieved by using reflections from three different orientations. An empirical absorption correction and other corrections were done using multi-scan SADABS. Structure solution, refinement and modeling were accomplished using the SHELXTL package (Bruker). The structure was obtained by full-matrix least-squares refinement of F^2 and the selection of appropriate atoms from the generated difference map.

2.3. Electrochemistry

Electrochemical measurements were recorded with an EG&G Princeton Applied Research Potentiostat/Galvanostat (Model 273A). The working electrode consisted of a platinum disk, 3 mm in diameter. A platinum mesh served as a counter electrode and a silver wire was used as a quasi reference electrode. All electrodes were polished with 0.05 μm alumina prior to measurements. The working and counter electrodes were separated using a vycor frit. Solutions were prepared with 100 mM TBAP electrolyte and degassed with argon for 20 min prior to each measurement. All reported standard potentials are versus SCE and were determined by adding ferrocene (taking $E^0_{Fc/Fc+} = 0.424$ V versus SCE in benzene) as an internal potential marker [15,16].

Bulk electrolysis to produce the radical cation was performed using a large area platinum mesh working electrode and a large area platinum counter electrode. The experimental design was the same as described above. The working electrode was biased at 50 mV above the first oxidation potential for 2 h using the Applied Research Potentiostat/Galvanostat. The oxidized solutions were transferred to quartz cells under ambient conditions and measurements were recorded immediately.

2.4. Spectroscopy

Unless otherwise stated, all experiments used optically dilute solutions (OD = 0.09–0.11) at room temperature. Luminescence samples in 1 cm^2 anaerobic quartz cells (Spectracell, FUV) were deoxygenated with argon prior to measurement. Low temperature experiments were accomplished by freezing the samples in NMR tubes and holding them under liquid nitrogen in a quartz dewar. Absorption spectra were measured with a Shimadzu scanning spectrophotome-

ter (UV-3101PC). Emission spectra were obtained with an Aminco-Bowman luminescence spectrometer (Series 2). The excitation was accomplished with a 250 W Xe lamp optically coupled to a monochromator (±2 nm) and the emission was collected at 90° and passed through a second monochromator (±2 nm). The luminescence was measured with a photomultiplier tube (PMT). Radiative quantum yields (Φ_r) were measured against $[Ru(bpy)_3](PF6)_2$ for which $\Phi_r = 0.062$ in CH_3CN, accurate to 10% [17], and calculated using the following equation [18,19]:

$$\Phi_{unk} = \Phi_{std}\left(\frac{I_{unk}}{A_{unk}}\right)\left(\frac{A_{std}}{I_{std}}\right)\left(\frac{\eta_{unk}}{\eta_{std}}\right)^2$$

where unk represents the sample, std the standard, Φ the radiative quantum yield, I the integrated emission intensity, A the absorbance at the excitation wavelength, and η the refractive index of the solvent.

Luminescence lifetimes were measured with an IBH time-correlated single photon counting (TCSPC) system equipped with an IBH Model TBX-04 Photon Detection Module. The excitation source for the TCSPC measurements was a pulsed LED (IBH NanoLED, 455 nm, 1.3 ns pulse duration or 403 nm, <200 ps pulse duration) with a repetition rate of 1 MHz. All data was analyzed by iterative reconvolution of the decay profile (10,000 counts at the peak channel) with the instrument response function using software provided by the instrument manufacturer.

Time-resolved absorption spectroscopy was performed using an LKS.60 nanosecond laser photolysis spectrometer. The excitation source was the unfocused 355 nm output of a Nd:YAG laser (Continuum Surelite I). Typical excitation energies were 2–3 mJ/pulse. Samples were continuously purged with a stream of high purity argon throughout the experiments. The data, consisting of either a single shot or a 10 shot average, were analyzed using Origin 7.0 (OriginLab Corporation).

It should be noted that all experiments performed in solution with light interaction resulted in sample degradation. Consequently, fresh samples were prepared for all physical measurements.

2.5. Synthesis of 1,5-dimethoxynaphthalene (2)

(a) [21,22] 1,5-Dihydroxynaphthalene (400 g, 2.50 mol), dimethylsulfate (476 ml, 5.02 mol), and potassium carbonate (346 g, 2.50 mol) were refluxed in 2 l of acetone for 2 days. Once cool, an equal volume of water was added and the solid collected by filtration. The crude product was purified by ethanol digestion (454 g, 97% yield). mp: 178–180 °C (lit., 181–183 °C [22] or 183–184 °C [21]). ^{1}H NMR (DMSO-d_6, 200 MHz, δ) 3.93 (s, 6H), 6.98 (d, J = 6.6 Hz, 2H), 7.39 (t, J = 6.6 Hz, 2H), 7.69 (d, J = 6.6 Hz, 2H). Mass: m/z 189.1 (positive ion mode).

2.6. Synthesis of 1,5-dimethoxy-4,8-di(4-methylbenzoyl)naphthalene (3)

(b) [22–24] Compound **2** (200 g, 1.06 mol) and anhydrous aluminum chloride (304 g, 2.29 mol) were cooled to 0 °C under nitrogen in 500 ml of 1,2-dichloroethane. *p*-Toluoylchloride (295 ml, 2.23 mol) was slowly added and the reaction mixture was stirred overnight at room temperature. Standard workup left a deep yellow solution that was concentrated by solvent evaporation. Petroleum ether was used to promote crystallization and the product was collected by filtration (208 g, 46% yield). mp: 246–248 °C. ^{1}H NMR (DMSO-d_6, 200 MHz, δ) 2.35 (s, 6H), 3.45 (2, 6H), 7.05 (d, J = 8.4 Hz, 2H), 7.24–7.45 (m, 10H). Mass: m/z 425.4 (positive ion mode).

2.7. Synthesis of 1,5-dihydroxy-4,8-di(4-methylbenzoyl)naphthalene (4)

(c) [20] Compound **3** (72 g, 169 mmol) was cooled to 0 °C under nitrogen in 500 ml of dichloromethane. Boron tribromide (79.8 ml, 844 mmol) was added slowly and the reaction was stirred 18 h at room temperature. The reaction was quenched with aqueous sodium bicarbonate and washed with dilute sodium hydroxide. The aqueous layer was neutralized with hydrochloric acid to give compound **4** (1.91 g, 3% yield) as an off white precipitate. It should be noted that washing with more concentrated base did not increase the yield of the substituted dihydroxynaphthalene. mp: 154–155 °C. ^{1}H NMR (DMSO-d_6, 200 MHz, δ) 2.33 (s, 6H), 6.76 (d, J = 7.4 Hz, 2H), 7.10 (d, J = 8.0 Hz, 2H), 7.21 (d, J = 8.2 Hz, 4H), 7.49 (d, J = 7.8 Hz, 4H), 10.52 (s, 2H). Mass: m/z 395.1 (negative ion mode). (e) [20] Compound **6** (573 mg, 1.37 mmol) was stirred in dichloromethane and water (1:1). The layers were separated and treated as above (see reaction (c)). Compound **4** was collected in 1% yield (5.7 mg) while compound **5** was recovered at 66% (380 mg). The reaction was also attempted with dichloromethane/$NaOH_{(aq)}$, acetone/water, and acetone/$NaOH_{(aq)}$. There was no improvement in yield. (f) Compound **5** (31.80 g, 83.6 mmol) was suspended in 300 ml of 6 M sodium hydroxide and refluxed for 18 h. Once cool, the reaction mixture was diluted (approx. 1 M NaOH), placed in an ice bath, and slowly acidified with concentrated hydrochloric acid [11]. The tan precipitate was collected by filtration, washed with excess water, and dried for 3 days in a vacuum oven (60 °C, <1 mmHg). Compound **4** was produced in 99% yield (33 g) and, with the exception of a slight color variance, was identical to the samples collected from reactions (c) and (d).

2.8. Synthesis of 6-(4-methylbenzoyl)-2-(4-methylphenyl)naphtho[1,8-b,c]furan-5-one (5)

The organic layer from **4**, procedure (c), was washed with dilute NaOH (2×), $NaHCO_3$ (2×), and water (3×). After dry-

ing over $MgSO_4$, the solvent was removed in vacuo providing compound **5** as a yellow-orange solid (47.54 g, 74% yield). mp: 212–214 °C. ^{1}H NMR ($CDCl_3$, 200 MHz, δ) 2.38 (s, 3H), 2.48 (s, 3H), 6.60 (d, J = 9.6 Hz, 1H), 7.20 (d, J = 8.0 Hz, 2H), 7.38–7.50 (m, 3H), 7.69–7.79 (m, 3H), 8.00 (d, J = 7.8 Hz, 3H). Mass: m/z 379.6 (positive ion mode).

2.9. Synthesis of 6-(4-methylbenzoyl)-5-hydroxy-2-(4-methylphenyl)naphtho[1,8-b,c]furylium perchlorate (6)

(d) [20] Compound **5** (500 mg, 1.41 mmol) was suspended in glacial acetic acid (10 ml) and excess perchloric acid (2 ml) was added slowly. The solution was refluxed for 10 min then cooled in an ice bath. Compound **6** precipitated as a red solid and was used without further purification or analysis (573 mg, 97% yield).

2.10. Synthesis of 1,5-di(benzyloxy)-4,8-di(4-methylbenzoyl)naphthalene (7a)

(g) [13] Tetrabutylammonium hydrogen sulfate (81.4 mg, 0.24 mmol), K_2CO_3 (2.98 g, 21.57 mmol), and KI (995 mg, 5.99 mmol) were dissolved in 50 ml H_2O. 4,8-Ditoluoyl-1,5-dihydroxynaphthalene (1.91 g, 4.79 mmol) and benzyl bromide (1.64 g, 9.59 mmol) was dissolved in 50 ml of 1,2-dichloroethane. The solutions were mixed quickly and refluxed under N_2 for 18 h. Once cool, the reaction solution was washed with saturated $NaHCO_3$ (2×) and H_2O (1×), dried over $MgSO_4$, filtered, and rotary evaporated to dryness. The resulting oil was taken up in a minimum amount of CH_2Cl_2 and dripped into cold petroleum ether. The crude product was recrystallized from MeOH and collected as a tan solid (961 mg, 35% yield). mp: 190–200 °C. ^{1}H NMR (DMSO-d_6, 200 MHz, δ) 2.27 (s, 6H), 4.80–5.03 (brdd, 4H), 6.82–7.43 (brm, 22H). Mass: m/z 575.7 (negative ion mode).

2.11. Synthesis of 1,5-di[(4-cyanobenzyl)oxy]-4,8-di(4-methylbenzoyl)naphthalene (7b)

(g) The reaction was run as described above with modification to the purification procedure. Reagents: tetrabutylammonium hydrogen sulfate (256.8 mg, 0.76 mmol), K_2CO_3 (9.41 g, 68.08 mmol), KI (3.14 g, 18.91 mmol), 4,8-ditoluoyl-1,5-dihydroxynaphthalene (6.00 g, 15.13 mmol), and 4-cyano benzyl bromide (5.96 g, 30.40 mmol). The crude product was digested in EtOH and collected as a tan solid (4.38 g, 46% yield). mp: 268–270 °C. ^{1}H NMR (DMSO-d_6, 200 MHz, δ) 2.33 (s, 6H), 4.97–5.14 (brdd, 4H), 7.10 (m, 16H), 7.69 (d, J = 8.0 Hz, 4H). ^{13}C ($CDCl_3$, 300 MHz, δ) 21.60, 69.94, 106.80, 111.77, 118.58, 124.22, 126.11, 128.04, 128.81, 129.39, 130.16, 132.09, 135.61, 140.37, 143.39, 153.98. Mass: m/z 628.2 (negative ion mode).

2.12. Synthesis of 2,7-di(4-cyanophenyl)-3,8-dihydroxy-3,8-di(4-methylphenyl)-2,3,7,8-tetrahydro-1,6-dioxapyrene (8)

(h) [25] Compound **7b** (2.00 g, 3.19 mmol) and tetrabutylammonium cyanide (2.49 g, 15.95 mmol) were dissolved in anhydrous CH_3CN (300 ml), protected from light, and refluxed under N_2 for 18 h. The solvent was removed and the residue dissolved in CH_2Cl_2. The organic phase was washed with saturated $NaHCO_3$ (2×) and H_2O (1×), dried over $MgSO_4$, filtered, and rotary evaporated to dryness. The crude product was a mixture of isomers and was used without further purification (∼1.5 g, 75% yield). ^{1}H NMR (DMSO-d_6, 200 MHz, δ) 2.07–2.46 (m, 6H), 5.39–5.78 (m, 2H), 6.41–7.71 (m, 20H).

2.13. Synthesis of 2,7-di(4-cyanophenyl)-3,8-di(4-methylphenyl)-1,6-dioxapyrene (9 or CN-diox)

(i) Compound **8** (∼1.5 g, 2.4 mmol) was dissolved in 100 ml of toluene and a catalytic amount of *p*-toluenesulfonic acid monohydrate. The reaction mixture was held under N_2 in the absence of light and refluxed for 2 days. A Dean-Stark trap was used to ensure anhydrous conditions. Once cool, the reaction mixture was held at 4 °C for 1 day followed by collection of the crude product as a red precipitate. The product was reprecipitated from hot CH_2Cl_2/$CHCl_3$ by addition of hot CH_3CN several times until the red, microcrystalline title compound was pure by HPLC (0.60 g, 43% yield). mp: 372–375 °C. ^{1}H NMR ($CDCl_3$, stabilized with $NaBH_4$, 300 MHz, δ) 2.36 (s, 6H), 6.10 (d, J = 5.4 Hz, 2H), 6.23 (d, J = 5.4 Hz, 2H), 7.03 (d, J = 5.4 Hz, 4H), 7.19 (d, J = 5.2 Hz, 4H), 7.25 (d, J = 6.0 Hz, 4H), 7.39 (d, J = 5.8 Hz, 4H). ^{13}C ($CDCl_3$, stabilized with $NaBH_4$, 300 MHz, δ) 21.33, 108.25, 111.25, 118.62, 119.29, 120.21, 128.96, 130.11, 130.23, 131.10, 131.45, 138.05, 138.32, 136.22, 151.69. Mass: m/z 590.6. Calculated for $C_{42}H_{26}N_2O_2 \cdot (1/4)CH_2Cl_2$: C 82.93, H 4.37. Found: C 82.90, H 4.40.

3. Results and discussion

3.1. Synthesis

1,5-Dihydroxy-4,8-di(4-methylbenzoyl)naphthalene (**4**) is the central compound in the present synthetic methodology. The hydroxyl groups on **4** provide a synthetic anchor from which numerous functionalities may be attached. Minyaeva and coworkers [20] have published the detailed synthesis of 4,8-dibenzoyl-1,5-dihydroxynaphthalene, which is closely related to our target molecule. Our approach was initially modeled after Minyaeva's synthesis (Scheme 1). Commercial grade 1,5-dihydroxynaphthalene (**1**) was protected by methylation of the hydroxyl groups to produce

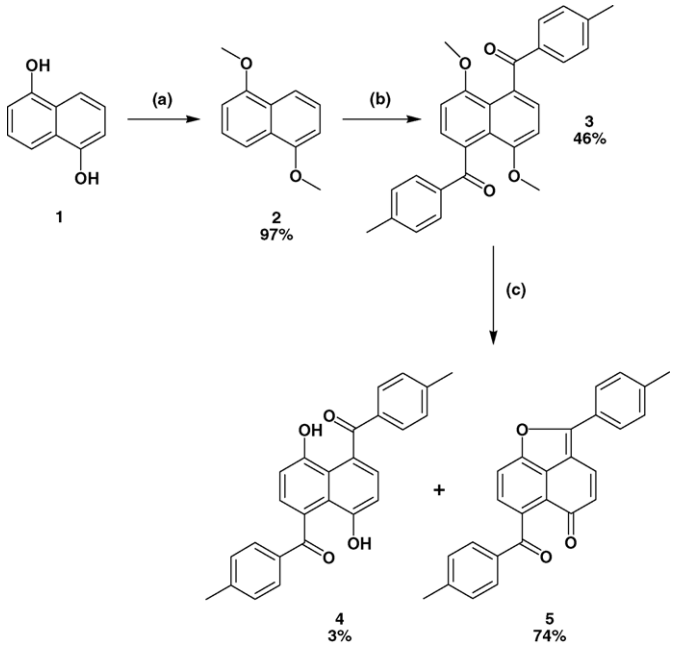

Scheme 1. Representation of the synthesis of 1,5-dihydroxy-4,8-di(4-methylbenzoyl)naphthalene (**4**) from 1,5-dihydroxynaphthalene (**1**).

1,5-dimethoxynaphthalene (**2**) in high yield [21,22]. Acylation of **2** presence of anhydrous aluminum chloride gave the expected product, 1,5-dimethoxy-4,8-di(4-methylbenzoyl) naphthalene (**3**) [22–24]. Deprotection of **3** progressed with excess boron tribromide to produce 1,5-dihydroxy-4,8-di(4-methylbenzoyl)naphthalene (**4**) in 3% yield and the corresponding methylenequinone, 6-(4-methylbenzoyl)-2-(4-methylphenyl)naphtho[1,8-b,c]furan-5-one (**5**), in 74% yield [20]. No attempts were made to isolate the partially demethylated hydroxymethoxydiketone. Also, the use of boron tribromide instead of aluminum chloride did not produce a significant change in our reaction yields as compared to Minyaeva's yields. Treatment of **5** with strong acid (Scheme 2) led to the naphtha-[1,8-b,c]furylium salt (**6**) in quantitative yield [20]. Subsequent hydrolysis of **6** produced **4** in 1% yield [20]. Although several solvent mixtures were evaluated, we were unable to come close to the 19% yield reported with the benzoyl derivative.

The transformation of the inevitable side-product, methylenequinone (**5**), to the desired product, dihydroxydiketone (**4**), is of considerable importance as a 1% yield falls well short of a synthetically useful method. Minyaeva indicates, and we agree, that the formation of methylenequinone is due to acid-catalyzed dehydration of the corresponding dihydroxydiketone. Under anhydrous and acidic conditions, dehydration is favored and formation of the methylenequinone predominates. By drastically reversing the reaction environment, the process is likely to proceed in the opposite direction. Following this logic, compound **5** was suspended in 6 M NaOH and refluxed for 18 h (Scheme 3). All extraction attempts resulted in loss of product due to inseparable suspensions. However, by simply precipitating the product from the diluted reaction mixture and washing with excess water we were able to obtain **4** in near quantitative yield [26]. Due to the hydrophylic nature of the substituted dihydroxynaphthalene, care must be taken to remove excess water. After

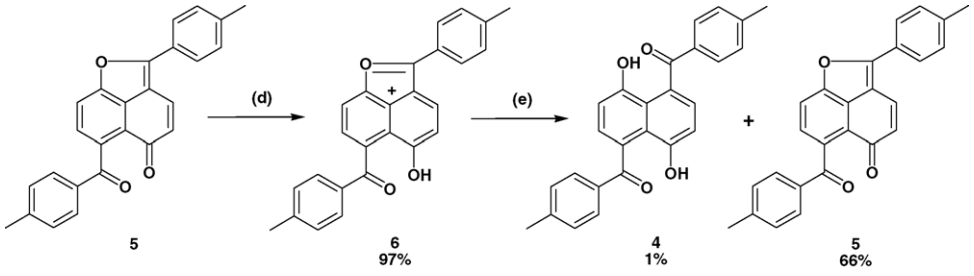

Scheme 2. Representation of the synthesis of 1,5-dihydroxy-4,8-di(4-methylbenzoyl)naphthalene (**4**) from 6-(4-methylbenzoyl)-2-(4-methylphenyl)naphtho [1,8-b,c]furan-5-one (**5**) using a two-step literature procedure.

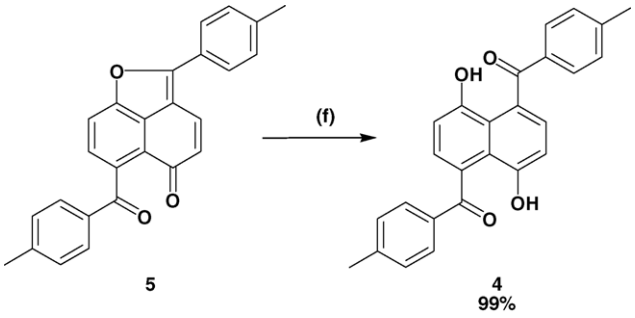

Scheme 3. Representation of the synthesis of 1,5-dihydroxy-4,8-di(4-methylbenzoyl)naphthalene (**4**) from 6-(4-methylbenzoyl)-2-(4-methylphenyl)naphtho[1,8-b,c]furan-5-one (**5**) using a modified one-step procedure.

vacuum drying at 60 °C for 3 days, 1,5-dihydroxy-4,8-di(4-methylbenzoyl)naphthalene (**4**) was collected in 99% yield.

Symmetrically substituted dibenzyl ethers (Scheme 4), 1,5-di(benzyloxy)-4,8-di(4-methylbenzoyl)naphthalene (**7a**) and 1,5-di[(4-cyanobenzyl)oxy]-4,8-di(4-methylbenzoyl) naphthalene (**7b**), were prepared in one step from **4** by a previously reported Williamson ether synthesis under phase transfer conditions [13]. It has been shown that *o*-benzyloxyphenyl ketones such as *o*-benzyloxybenzophenone [27], α-(*o*-benzyloxyphenyl)acetophenone [28], and related compounds [13,28–30] undergo efficient photoinduced hydrogen abstraction (ε-hydrogen abstraction in the case of α-(*o*-benzyloxyphenyl)acetophenone) to produce biradicals that spontaneously cyclize in high yield (Scheme 5). Photo-initiated (450 W Hg lamp, benzene) ring closure via a similar excited state intramolecular ε-hydrogen abstraction was unsuccessful for both **7a** and **7b**. The excited state absorption spectrum of 1,5-di(benzyloxy)-4,8-di(4-methylbenzoyl)naphthalene (**7a**) is shown in Fig. 2. The data reveals a broad transient band centered near 430 nm with a lifetime of 25 ± 2 μs in deoxygenated benzene. Related *o*-alkoxyphenyl and *o*-benzoyloxyphenyl ketones that produce biradical transient species show decay rates on the order of 1–50 ns [30–32]. Excited state absorption studies of naphthalene have shown both singlet π,π^* (<100 ns) and triplet π,π^*

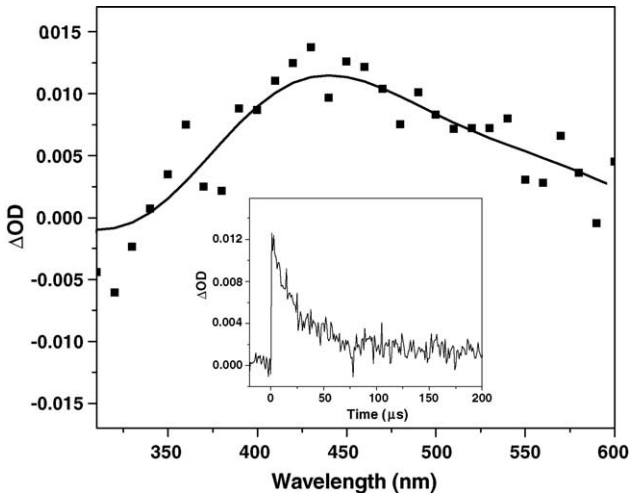

Fig. 2. Transient absorption spectrum of 1,5-di(benzyloxy)-4,8-di(4-methylbenzoyl)naphthalene (**7a**). The experiment was performed in deoxygenated benzene at room temperature with 355 nm pulsed excitation. (Inset) Kinetic trace of *CN-diox* (**9**) at 430 nm.

(>100 ns) species [33]. Based on this data, the excited state of 1,5-di(benzyloxy)-4,8-di(4-methylbenzoyl)naphthalene (**7a**) is assigned to the π,π^* triplet, not the 1,7-biradical. The absence of the biradical intermediate effectively prevents the synthesis of 1,6-dioxapyrenes by this methodology.

An alternative route to the photochemical process is shown in Scheme 4. Base-catalyzed ring closure of **7b** using tetrabutylammonium cyanide and anhydrous acetonitrile resulted in the corresponding hydrated 1,6-dioxapyrene in 75% yield [25]. The analogous reaction using **7a** resulted in no reaction as only unreacted starting material was recovered. These results are not surprising as related work has shown that the inductive properties of the pendant phenyl group directly affect the efficiency of the ring closure reaction [33]. In this process, the abstraction of the α-proton (in relation to the ether) is favored by functional groups that delocalize the incipient negative charge (i.e. electron withdrawing groups). Our results agree with this observation because the phenyl derivative imparts no charge delocalization and no reaction yield

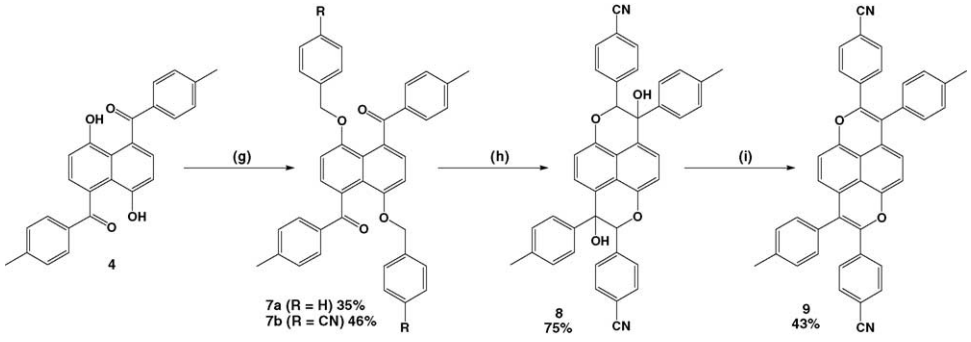

Scheme 4. Representation of the synthesis of 2,7-di(4-cyanophenyl)-3,8-di(4-methylphenyl)-1,6-dioxapyrene (**9** or *CN-diox*) from 1,5-dihydroxy-4,8-di(4-methylbenzoyl)naphthalene (**4**).

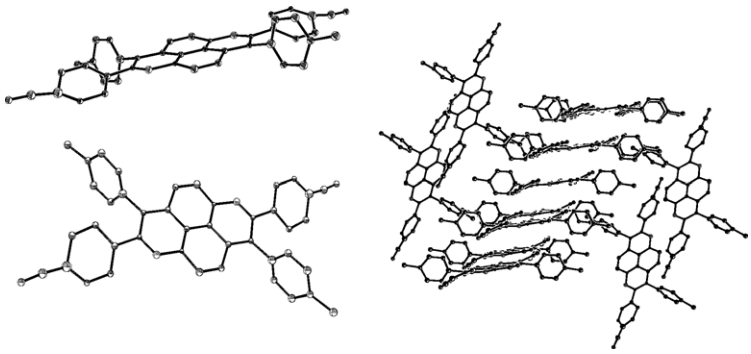

Fig. 3. X-ray structures for *CN-diox* (**9**).

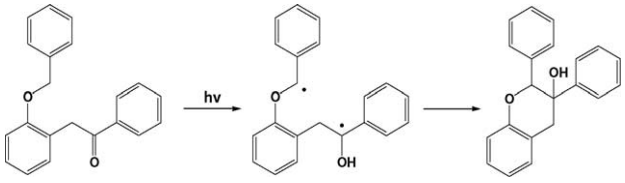

Scheme 5. Simplified representation of the photocyclization of α-(*o*-(benzyloxyphenyl)acetophenone) via the 1,6-biradical intermediate [27].

while the cyano-substituted phenyl derivative maintains a large delocalization effect and high reaction yield. The transformation of **8** to the desired 2,7-di(4-cyanophenyl)-3,8-di(4-methylphenyl)-1,6-dioxapyrene (**9** or *CN-diox*), proceeded in 43% yield via acid-catalyzed dehydration under Dean-Stark conditions. The crude product was dissolved in hot $CH_2Cl_2/CHCl_3$ and reprecipitated by slow addition of hot CH_3CN. The procedure was repeated several times until the red, microcrystalline compound (**9** or *CN-diox*) was pure by HPLC.

3.2. Crystallography

The TEP representation of *CN-diox* (**9**) is displayed in Fig. 3. The *core* (i.e. only the 1,6-dioxapyrene) shows a slight twist that is not present in *Diox* (**11**) [6]. Both oxygens are out of the plane (one up and one down) by 0.1 Å from the center of each oxygen or 8.9° using the inner dihedral angle. In direct comparison, *Diox* (**11**) shows no deviation from a planer structure. The cyanophenyl and methylphenyl substituents are at dihedral angles of 22.7° and 82.6°, respectively, from the *core*. The extended X-ray structure shows repeating *CN-diox* (**9**) in an off-center columnar arrangement. Each end of the *CN-diox* (**9**) in the column is adjacent to a perpendicular *CN-diox* (**9**). The resultant phenyl cage maintains one CH_2Cl_2 between four substituted phenyl rings.

3.3. Electrochemistry

The electrochemical data of *CN-diox* (**9**), *Alkyl-diox* (**10**), and *Diox* (**11**) in benzonitrile is summarized in Table 1. A representative cyclic voltammogram of a benzonitrile solution of *CN-diox* (**9**) is given in Fig. 4. All reported standard potentials are versus SCE and were determined by using ferrocene as an internal potential marker [15,16]. Reduction potentials were not investigated as they were not observed in the solvent window and the low solubility of *CN-diox* (**9**) limited the choice of other solvent systems. All three 1,6-dioxapyrenes had two oxidation waves. The first oxidation wave was 0.571 V for *CN-diox* (**9**), 0.308 V for *Alkyl-diox* (**10**), and 0.529 V for *Diox* (**11**). It is important to note that the first oxidation potentials for *CN-diox* (**9**) and *Diox* (**11**) were similar. This data suggests that the core of the 1,6-dioxapyrene remains electronically unaffected by the addition of pendant phenyl groups. Analysis of ΔE_p and $i_{p\,ox}/i_{p\,red}$ values indicated the first oxidation waves for each 1,6-dioxapyrene were reversible. ΔE_p's, the difference between the peaks of the forward and reverse sweeps, for *CN-diox* (**9**), *Alkyl-diox* (**10**), and *Diox* (**11**) were between was 0.082 and 0.084 V.

Table 1
Electrochemical data at room temperature in benzonitrile

Solvent	$^1E_{1/2}$ [a] (V)	ΔE_p [b] (V)	$i_{p\,ox}/i_{p\,red}$ [c]	$^2E_{1/2}$ [a] (V)	ΔE_p (V)	$i_{p\,ox}/i_{p\,red}$	$E_{1/2\,red}$ [e] (V)
9	0.571	0.084	1.03	0.989[d]	–	–	0.061
10	0.308	0.082	1.55	0.686	0.125	2.74	−0.091
11	0.529	0.084	1.56	1.026[d]	–	–	−0.187

[a] Degassed benzonitrile, 100 mM tetrabutylammonium perchlorate, at 50 mV/s.
[b] Ferrocene displayed a ΔE_p of 0.80 ± 5 V under our experimental conditions when not significantly overlapping other waves.
[c] A completely reversible system should have an $i_{p\,ox}/i_{p\,red}$ of 1.00.
[d] E_{ox} reported instead of $E_{1/2}$ due to irreversibility.
[e] Represents the peak of a new reduction wave after performing repeated oxidations.

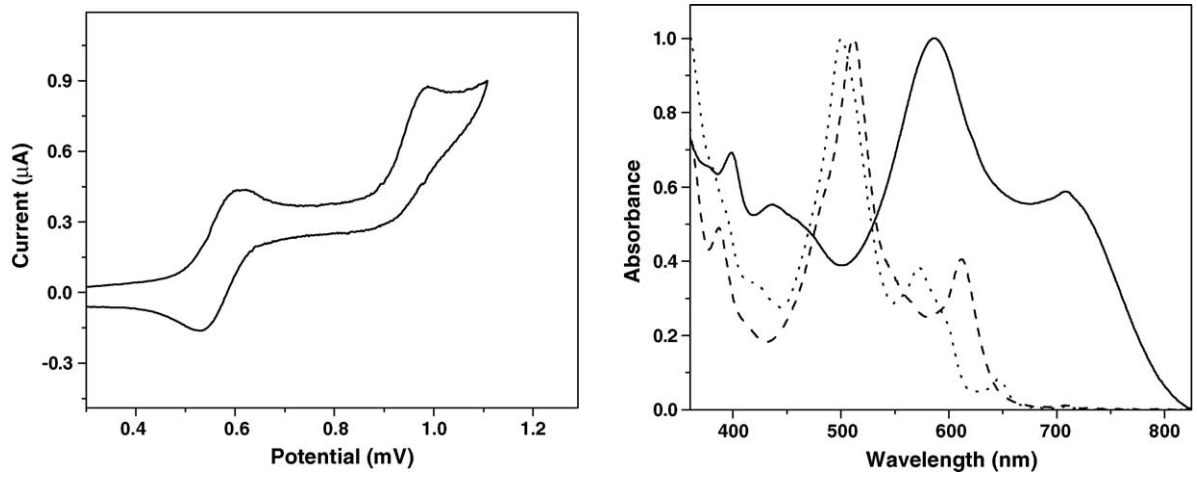

Fig. 4. (Left) Cyclic voltammogram of *CN-diox* (**9**). The experiment was performed in benzonitrile (0.1 M $TBAPF_6$) at a scan rate of 50 mV/s. (Right) Electronic spectra of the electrochemically generated radical cation of *CN-diox* (**9**, solid line), *Alkyl-diox* (**10**, dashed line), and *diox* (**11**, dotted line) in benzonitrile.

Ferrocene displayed a ΔE_p of 0.080 V under our experimental conditions. Although all ΔE_p measurements were higher than the accepted 0.059 V for reversible processes [34], direct comparison of the 1,6-dioxapyrenes to ferrocene (which is known to have reversible one electron oxidation behavior [15,16]) illustrates the reversibility of the oxidation waves. In a separate analysis, $i_{p\,ox}/i_{p\,red}$ was calculated to be 1.03 for *CN-diox* (**9**), 1.55 for *Alkyl-diox* (**10**), and 1.56 for *Diox* (**11**). Under ideal conditions, a completely reversible process will show an $i_{p\,ox}/i_{p\,red}$ of 1.00.

CN-diox (**9**), *Alkyl-diox* (**10**), and *Diox* (**11**) maintained a second oxidation wave at 0.989, 0.686, and 1.026 V, respectively. The second oxidation wave for each 1,6-dioxapyrene showed irreversible behavior. The reverse wave was not visible for *CN-diox* (**9**) and *Diox* (**11**) and consequently neither ΔE_p nor $i_{p\,ox}/i_{p\,red}$ values could be determined. *Alkyl-diox* (**10**) had a minimal reverse wave and both ΔE_p (0.125 V) and $i_{p\,ox}/i_{p\,red}$ (2.74) values indicated irreversible processes. The nature of the irreversibility (i.e. electrochemical or chemical reactions, or a combination of both) was not investigated. In all cases, however, a new reduction wave was observed during the reverse sweep. This wave always appeared at lower potential than the first oxidation wave and was only seen after the cell potential was raised beyond the second oxidation potential. This suggests chemical degradation as a source of irreversibility, although it does not eliminate electrochemical irreversibility.

Fig. 4 displays the absorption spectra for the radical cations of *CN-diox* (**9**), *Alkyl-diox* (**10**), and *Diox* (**11**) in benzonitrile. Photoluminescence was not detectable for any of the radical cations. The radical species were electrochemically generated as described in the experimental section and were found to be stable under ambient conditions for several hours. The electronic spectra of *Alkyl-diox* (**10**) and *Diox* (**11**) show two main absorption bands with absorption maxima near 500 and 600 nm. The spectrum of *CN-diox* (**9**) also reveals two main absorption bands; however the transitions were significantly lower in energy, near 580 and 700 nm. Although the oxidation potentials are similar, the addition of a cyanophenyl group to the 1,6-dioxapyrene core lowers the excited state transitions of the radical cation of *CN-diox* (**9**).

3.4. Photophysical properties

Fig. 5 displays the absorption spectra of *CN-diox* (**9**), *Alkyl-diox* (**10**), and *Diox* (**11**) in THF (all solvents displayed similar absorption features). The electronic spectrum of *Alkyl-diox* (**10**) shows a broad absorption band with a maximum at 370 nm and a molar absorption coefficient of 11,000 $M^{-1}\,cm^{-1}$. The electronic spectrum of *Diox* (**11**) reveals a broad absorption band with three clear peaks of 360, 395, and 420 nm having molar absorption coefficients of 7600, 4500 and 4500 $M^{-1}\,cm^{-1}$, respectively. The spectrum of *CN-diox* (**9**), however, reveals unique behavior in compar-

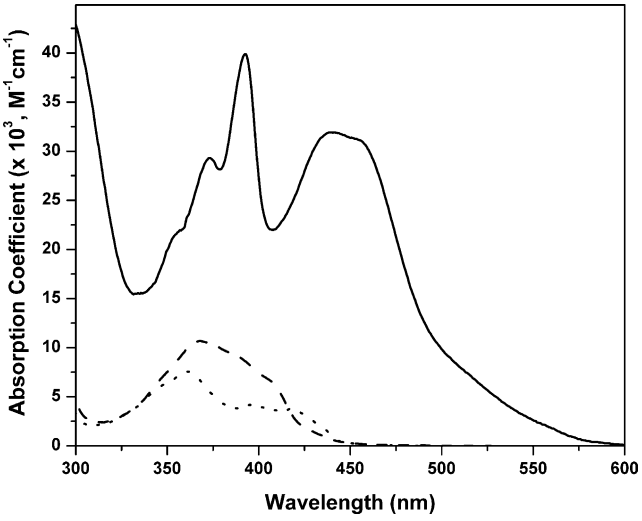

Fig. 5. Electronic spectra of *CN-diox* (**9**, solid line), *Alkyl-diox* (**10**, dashed line), and *Diox* (**11**, dotted line) in THF.

ison to the unsubstituted 1,6-dioxapyrenes. *CN-diox* (**9**) has two main areas of absorption; a low energy, broad band with an absorption maximum at 440 nm and a molar absorption coefficient of 32,000 M^{-1} cm^{-1} and a higher energy band with a distinct vibrational structure. The latter has three clear bands, red shifted but similar to pyrene, and an absorption maximum at 390 nm and a molar absorption coefficient of 41,000 M^{-1} cm^{-1}. These data indicate a significant distortion of the *typical* 1,6-dioxapyrene core. First, the appearance of a lower energy absorption band without significant change in the oxidative properties indicates a lowering of the LUMO in *CN-diox* (**9**) as compared to *Alkyl-diox* (**10**) and *Diox* (**11**). Second, the pyrene-like vibrational structure of the higher energy absorption band suggests a higher degree of aromaticity within *CN-diox* (**9**).

The luminescence maxima, quantum yields, and excited state lifetimes of *CN-diox* (**9**), *Alkyl-diox* (**10**), and *Diox* (**11**) in solvents of different polarity are summarized in Table 2 [35]. The emission spectra of *CN-diox* (**9**), *Alkyl-diox* (**10**), and *Diox* (**11**) in THF are shown in Fig. 6. The photoluminescence was normalized to 1 and *CN-diox* (**9**, solid line) shows a clear THF Raman band near 500 nm that should not be misinterpreted as analyte luminescence. The emission spectra of *Alkyl-diox* (**10**) and *Diox* (**11**) show structured bands with maximum intensities at 497 and 487 nm, respectively,

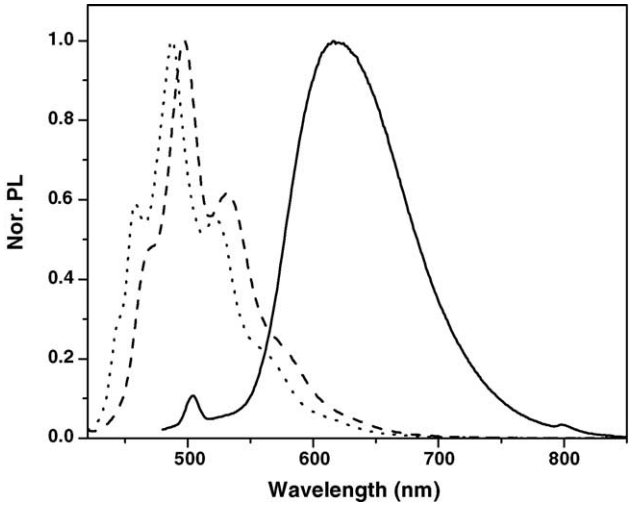

Fig. 6. Normalized photoluminescence spectra of *CN-diox* (**9**, solid line), *Alkyl-diox* (**10**, dashed line), and *Diox* (**11**, dotted line) in THF at 23 °C. The excitation wavelengths were 440, 370, and 360 nm, respectively.

while *CN-diox* (**9**) has a broad emission band centered near 619 nm. As shown in Table 2, both *Alkyl-diox* (**10**) and *Diox* (**11**) show small to moderate solvent dependence on emission maxima with no clear polarity trend. *CN-diox* (**9**), on the other hand, has a 50 nm solvatochromic shift, increasing

Table 2
Spectroscopic and photophysical data of *CN-diox* (**9**), *Alkyl-diox* (**10**), and *Diox* (**11**) in solvents of increasing polarity

Solvent (dielectric)	Em. λ_{max} (nm)[a]			$^1\tau$ (ns)[b]			Φ_r[c]			k_f ($\times 10^9$ s^{-1})	k_d ($\times 10^9$ s^{-1})
	9	**10**	**11**	**9**	**10**	**11**	**9**	**10**	**11**	**9**	**9**
Toluene (2.4)	593	498	489	1.39	6.93	6.97	0.010			0.0072	0.71
					2.41	3.39		0.044			
									0.115		
$CHCl_3$ (4.8)	619	476	493	0.92	7.27	4.82	0.011			0.012	1.08
					2.28	1.78		0.011			
					0.51	0.44			0.012		
THF (7.6)	619	497	487	0.78	7.09	6.77	0.011			0.014	1.27
					3.40	3.41		0.059			
									0.082		
CH_2Cl_2 (9.1)	629	500	490	0.69	7.17	6.54	0.0071			0.010	1.44
					2.73	3.06		0.069			
									0.094		
$C_2H_4Cl_2$ (10.7)	625	466	490	0.68	6.26	7.16	0.011			0.016	1.45
					2.51	3.18		0.10			
					0.31				0.084		
Acetone (20.1)	632	497	487	0.50	6.03	5.76	0.0055			0.010	1.99
					2.74	3.14		0.039			
									0.069		
DMF (37)	640	499	489	0.38	8.47	7.47	0.0036			0.011	2.62
					3.59	3.32		0.069			
									0.085		
DMSO (45)	644	500	491	0.36	9.61	8.49	0.0034			0.0083	2.77
					4.03	3.72		0.088			
									0.13		

[a] Represents the maximum of the largest emission peak.
[b] TCSPC using 455 nm or 403 excitation (pulsed LED) and iterative reconvolution with an error of less than 5%.
[c] $Ru(bpy)_3^{2+}$ in ACN ($\Phi = 0.064$) was used an actinometer in all cases (error = ±10%).

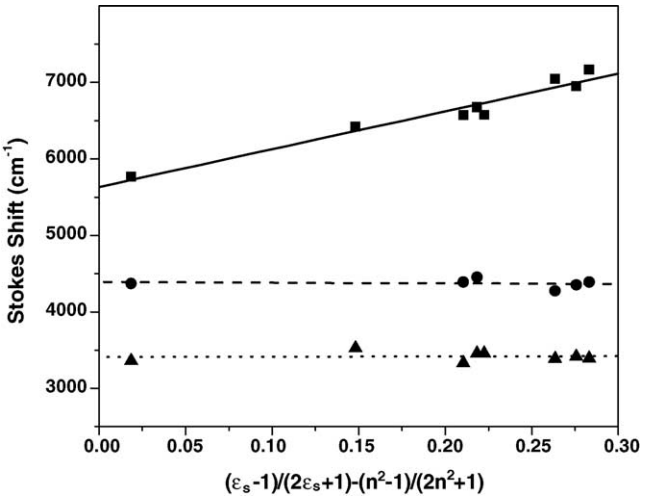

Fig. 7. Relationship of the Stokes shift and Lippert-Mataga polarity parameter for *CN-diox* (**9**, ■, solid line), *Alkyl-diox* (**10**, ●, dashed line), and *Diox* (**11**, ▲, dotted line) in the eight solvents listed in Table 2. Two solvents were removed from the analysis of *Alkyl-diox* (**10**) due to broad emission spectra.

systematically from 593 nm in toluene to 644 nm in DMSO. These data suggest a charge transfer nature to the excited state of the cyano-substituted 1,6-dioxapyrene derivative.

The solvatochromic response of *CN-diox* (**9**) to photoexcitation was further characterized by analysis of the Stokes shift and Lippert-Mataga polarity parameter:

$$\bar{\nu} = \frac{1}{4\pi hc\varepsilon_0}\frac{(\Delta\mu)^2}{\alpha^3}\left(\frac{\varepsilon_s - 1}{2\varepsilon_s + 1} - \frac{n^2 - 1}{2n^2 + 1}\right) + C$$

where $\bar{\nu}$ is the Stokes shift in wavenumbers, h the Plank's constant, c the speed of light, ε_0 the permittivity of free space, $\Delta\mu$ the change in the dipole moment upon excitation, α^3 the molecule's volume [36], ε_s the solvent dielectric constant, and n the solvent refractive index [37–42]. This relationship quantifies the change in dipole between the ground state and excited state of a molecule and, when used with the calculated ground state dipole [36], the magnitude of the excited state dipole moment may be estimated. The Lippert-Mataga correlations of *CN-diox* (**9**), *Alkyl-diox* (**10**) and *Diox* (**11**) are shown in Fig. 7. The slopes of *Alkyl-diox* (**10**) and *Diox* (**11**) are nearly zero, indicating small changes in dipole for each molecule ($\leq 6.677 \times 10^{-30}$ C m, or ∼2.00 D, as calculated from the Lippert-Mataga relationship). *CN-diox* (**9**), however, displays a slope of 4940.6 cm^{-1} ($R^2 = 0.95$). Using the volume of 530.307 $Å^3$ from molecular modeling, $\Delta\mu = 7.610 \times 10^{-29}$ C m or 22.81 D. The ground state dipole from molecular modeling was 0.004889 D, thus the excited state dipole is ∼22.81 D. This data further supports the existence of a polar excited state for *CN-diox* (**9**), a distinctive property as compared to *Alkyl-diox* (**10**) and *Diox* (**11**).

The unique properties of *CN-diox* (**9**) are also observed with the luminescence quantum yields and excited state lifetimes. *CN-diox* (**9**), *Alkyl-diox* (**10**), and *Diox* (**11**) show a significant solvent dependence (Φ_f range of 0.003–0.127) on emission quantum yield, yet there is no clear trend for *Alkyl-diox* (**10**), and *Diox* (**11**). *CN-diox* (**9**) displays a general decrease of quantum yield from nonpolar ($\Phi_f = 0.010$ in toluene) to polar environments ($\Phi_f = 0.0034$ in DMSO). *Alkyl-diox* (**10**) and *Diox* (**11**) maintain multiple exponential fluorescence decays in all solvents [43]. In general, the unsubstituted 1,6-dioxapyrenes have double exponential fluorescence decays with a long component of approximately 5–8 ns and a short component of 2–4 ns. Again, *CN-diox* (**9**) displays uncharacteristic behavior with single exponential lifetimes in all solvents [43]. Furthermore, the excited state lifetimes of *CN-diox* (**9**) measurably decrease from 1.39 ns in toluene (nonpolar) to 0.36 ns in DMSO (polar). The derived k_d and k_f values for *CN-diox* (**9**, Table 2) highlight an interesting trend. Specifically, the nonradiative decay rate, k_d, is continuously increased from nonpolar to polar solvents. Furthermore, there is no clear trend with respect to the radiative decay rates, k_f. As noted earlier, *CN-diox* (**9**) decomposes/reacts with continuous exposure to light, both in the presence and absence of oxygen. The increase in k_d suggests the destructive pathway may be enhanced in polar environments. Further work is underway to identify and possibly control the excited state decomposition.

3.5. Summary

A symmetrically substituted 2,3,7,8-tetraaryldioxapyrene, 2,7-di(4-cyanophenyl)-3,8-di(4-methylphenyl)-1,6-dioxapyrene (**9** or *CN-diox*), was synthesized in seven steps from 1,5-dihydroxynaphthalene (**1**). The first notable transformation is the alkaline treatment of **5** to produce **4** in one step with a 99% yield, an improvement of 80% compared to the acidic, two-step literature method for preparing 4,8-dibenzoyl-1,5-dihydroxynaphthalene. The second important sequence is the base-catalyzed ring closure followed by the acid-catalyzed dehydration to produce *CN-diox* (**9**). The complete synthesis represents a new route for preparing tetraaryl-1,6-dioxapyrenes. Crystal structure and electrochemical analysis were performed to directly compare the properties of *CN-diox* (**9**) to previously reported dioxapyrene derivatives, specifically 1,6-dioxapyrene (**11** or *Diox*) and 3,8-diethyl-5,10-dimethyl-1,6-dioxapyrene (**10** or *Alkyl-diox*). Crystallography revealed the dioxapyrene core oxygens were out-of-plane by 8.9°, using the inner dihedral angle, and the dihedral angle between the cyanophenyl and the central structure was 22.7°. Electrochemistry showed similar oxidative behavior for all derivatives with notably lower energy transitions in the corresponding spectroelectrochemical absorption spectra. Both data suggest similar electronic structure for the 1,6-dioxapyrene core and a lowering of the LUMO by covalent attachment of an electron accepting group. Optical spectroscopy studies were performed to evaluate the potential of the 1,6-dioxapyrenes as fluorescent probes. *CN-diox* revealed broad absorption and emission properties that were red shifted with respect to the two model compounds, *Diox* (**11**) nor *Alkyl-diox* (**10**). The luminescence of *CN-diox* (**9**) was found to be solvatochromic

(λ_{max} = 619–644 nm) with single exponential lifetimes of less than 1.3 ns and an excited state dipole moment of ~22.81 D. Neither *Diox* (**11**) nor *Alkyl-diox* (**10**) showed solvatochromic properties. These date indicate the presence of a charge transfer excited state in *CN-diox* (**9**). Continuing efforts will focus on synthesizing alternative donor/accepter derivatives to systematically study the spectroscopic properties of this new class of 1,6-dioxapyrene.

Acknowledgements

We thank Javier Santos for sharing the base-catalyzed ring closure procedure, Daniel A. Scheiman for assistance with purification, and Faysal Ilhan and Mary Ann Meador for helpful discussions. DST is supported by a NASA cooperative agreement (NCC3-1089). This research was supported by the Vehicle Systems Project and Internal Research and Development Fund at the NASA Glenn Research Center.

References

[1] J.-P. Buisson, P. Demerseman, J. Heterocycl. Chem. 27 (1990) 2213.
[2] J.B. Christensen, J. Larsen, I. Johannsen, K Bechgaard, Synth. Met. 41–43 (1991) 2311.
[3] J.B. Christensen, I. Johannsen, K. Bechgaard, J. Org. Chem. 56 (1991) 7055.
[4] M.B. Mortensen, A. Schlütel, J. Sørensen, J.B. Christensen, Acta Chem. Scand. 51 (1997) 807.
[5] J.B. Christensen, K. Bechgaard, J. Heterocycl. Chem. 40 (2003) 757.
[6] J.-P. Bideau, M. Cotrait, J.-P. Buisson, P. Demerseman, Acta Crystallogr. C 48 (1992) 1129.
[7] N. Thorup, M. Hjorth, J.B. Christensen, K. Bechgaard, Synth. Met. 55–57 (1993) 2069.
[8] N. Platzer, J.-P. Buisson, P. Demerseman, J. Heterocycl. Chem. 29 (1992) 1149.
[9] J.-P. Buisson, J. Kotzyba, J.-P. Lièvremont, P. Demerseman, N. Platzer, J.-P. Bideau, M. Cotrait, J. Heterocycl. Chem. 30 (1993) 739.
[10] K. Bechgaard, K. Lerstrup, M. Jørgensen, I. Johannsen, J. Christensen, J. Larsen, Mol. Cryst. Liq. Cryst. 181 (1990) 161.
[11] S.A. Tucker, W.E. Acree Jr., M. Zander, P. Demerseman, J.-P. Buisson, Appl. Spectrosc. 47 (1993) 317.
[12] M. Kataoka, T. Sato, J. Heterocycl. Chem. 36 (1999) 1323.
[13] M. Abdul-Aziz, J.V. Auping, M.A. Meador, J. Org. Chem. 60 (1995) 1303.
[14] In this case, "unsubstituted" refers to the absence of electron accepting groups. Clearly Alkyl-diox (**10**) has methyl and ethyl functional groups.
[15] J.D. Debad, J.C. Morris, V. Lynch, P. Magnus, A.J. Bard, J. Am. Chem. Soc. 118 (1996) 2374.
[16] J.D. Debad, J.C. Morris, P. Magnus, A.J. Bard, J. Org. Chem. 62 (1997) 530.
[17] J.V. Casper, T.J. Meyer, J. Am. Chem. Soc. 105 (1983) 5583.
[18] N.H. Damrauer, T.R. Boussie, M. Devenney, J.K. McCusker, J. Am. Chem. Soc. 109 (1997) 8253.
[19] J.N. Demas, G.A. Crosby, J. Phys. Chem. 75 (1971) 991.
[20] V.V. Mezheritskii, R.V. Tyurin, L.G. Minyaeva, Russ. J. Org. Chem. 37 (2001) 513.
[21] W.H. Benthey, R. Robinson, C. Weizmann, J. Chem. Soc. (1907) 104.
[22] J.E. Corrie, T.G. Papageorgiou, J. Chem. Soc., Perkin Trans. 1 (1996) 1583.
[23] H.E. Fierz-David, G. Jaceard, Helv. Chim. Acta 11 (1928) 1042.
[24] H. Ritter, R. Thorwirth, Makromol. Chem. 194 (1993) 1469.
[25] J. Santos, M.A. Meador, in preparation.
[26] The reversibility of this reaction in acidic solutions is an area of concern when precipitating with concentrated hydrochloric acid. Slow addition of the acidic solution with constant stirring until the reaction mixture was just below pH 7 minimized the back reaction.
[27] P.J. Wagner, M.A. Meador, J.C. Scaiano, J. Am. Chem. Soc. 106 (1984) 7988.
[28] M.A. Meador, P.J. Wagner, J. Org. Chem. 50 (1985) 420.
[29] P.J. Wagner, M.A. Meador, B.-S. Park, J. Am. Chem. Soc. 112 (1990) 5199.
[30] P.J. Wagner, Acc. Chem. Res. 22 (1989) 83.
[31] P.J. Wagner, J.-S. Jang, J. Am. Chem. Soc. 115 (1993) 7914.
[32] P.J. Wagner, M.A. Meador, B. Zhou, B.-S. Park, J. Am. Chem. Soc. 113 (1991) 9630.
[33] R. McNeil, J.T. Richards, J.K. Thomas, J. Phys. Chem. 74 (1970) 2290.
[34] L.R. Faulkner, A.J. Bard, in: A.J. Bard (Ed.), Electroanalytical Chemistry, vol. 10, Marcel Dekker, New York, 1977.
[35] Solvents were chosen to cover a wide range of molecular environments, from toluene with a dielectric of 2.4 to DMSO with a dielectric of 45. Protic/nonprotic solvent complications were not an issue in the present work because the chromophores likely do not possess basic character. Also, although mixing of aromatic and nonaromatic solvents should be avoided when working with charge transfer compounds, there were no significant deviations in the current work. For further discussion see: J. Catalán, J. Org. Chem. 62 (1997) 8231.
[36] Molecular modeling was accomplished using HyperChem (2002) by Hypercube, Inc. Initial energy minimization used the AMBER force field while ground state dipole and volume calculations used MM+. Volume calculations used a solvent probe radius of 0.1 Å.
[37] F. Würthner, S. Ahmed, C. Thalacker, T. Debaerdemaeker, Chem. Eur. J. 8 (2002) 4742.
[38] E.L. Mertz, V.A. Tikhomirov, L.I. Krishtalik, J. Phys. Chem. A 101 (1997) 3433.
[39] E. Lippert, W.Z. Lüder, Z. Phys. Chem. (Frankfurt) 1962 (1962) 60.
[40] E. Lippert, Elektrochemistry 61 (1957) 962.
[41] N. Mataga, Y. Kaifu, M. Koizumi, Bull. Chem. Soc. Jpn. 28 (1955) 690.
[42] N. Mataga, Y. Kaifu, M. Koizumi, Bull. Chem. Soc. Jpn. 29 (1956) 465.
[43] The identification of multiple fluorescence decays for *Diox* (**11**) and *Alkyl-diox* (**10**) is surprising and requires additional discussion. Non-super imposable excitation spectra were recorded for *Diox* (**11**) and *Alkyl-diox* (**10**), which indicated the presence of fluorescent impurities. Upon prolonged irradiation, the excitation spectra became increasingly distorted. This data indicates an increase in the amount of fluorescent impurity during photoexcitation. It is reasonable to suggest that one or more of the degradation products are responsible for the additional fluorescence. Furthermore, because the impurity is coming from the decomposition of the sample, it is not possible to eliminate its effect. For *Diox* (**11**) and *Alkyl-diox* (**10**), the degradation product emission overlaps the sample emission and is recorded as multiple exponential fluorescence decays. For *CN-diox* (**9**), however, the degradation product emission does not overlap the sample emission and the fluorescence is recorded as a single exponential lifetime.